

ORIGINAL ARTICLE



Seismic performance assessment of self-centering hybrid coupled walls: an 8-story case study structure

Mojtaba Farahi¹ | Fabio Freddi¹ | Massimo Latour²

Correspondence

Dr. Mojtaba Farahi
University College London
Chadwick Building, Gower Street,
Room 120
London WC1E 6BT
Email: mojtaba.farahi@ucl.ac.uk

¹ Department of Civil, Environmental & Geomatic Engineering,
University College of London, London, UK

² Department of Civil Engineering,
University of Salerno, Salerno, Italy

Abstract

In response to the demand for resilient structures, a variety of innovative structural solutions have been recently introduced to reduce residual deformations and expedite the repair of structures subjected to earthquakes. This paper discusses the seismic performance of a self-centering lateral load-resisting system developed with the intent of diminishing earthquake-induced damage and residual deformations. The proposed solution is composed of a reinforced concrete (RC) shear wall coupled to two steel side columns with coupling beams featuring a friction-damped self-centering mechanism. The intended system is referred as Self-Centering Hybrid Coupled Wall (SC-HCW). The applied self-centering mechanism is aimed at reducing earthquake-induced residual deformations. Limited residual deformations facilitate the repair of SC-HWs after severe earthquakes, which improves the seismic resilience of the structure. The seismic performance of a SC-HCW is examined and compared with that of a conventional hybrid coupled wall (HCW). Nonlinear static and Incremental Dynamic Analyses (IDAs) are conducted on these archetypes. The outcomes elaborate the efficiency of the SC-HCW in minimizing earthquake-induced residual deformations.

Keywords

Hybrid Coupled Wall Systems, Self-Centering, Reinforced Concrete Walls, Shear Links, Seismic Performance

1 Introduction

The superior strength and stiffness of reinforced concrete (RC) coupled walls make them a proper choice as lateral load-resisting systems for medium- to high-rise structures in seismic-prone regions [1, 2]. However, significant damage to the coupling beams may result in large residual deformations after severe earthquakes [3-6]. Large earthquake-induced residual deformations do not allow an easy and fast repair of the structure leading to significant direct (e.g., repair cost) and indirect (e.g., downtime) socioeconomic losses. In this context, there is an eminent need for 'seismic-resilient' solutions that provide large ductility and energy dissipation capacity in conjunction with self-centering (SC) capability to facilitate the required structural repairs.

To improve the ductility and energy dissipation capacity of coupled systems, Zona *et al.* [7, 8] proposed an innovative steel-concrete hybrid structural solution. In this configuration, named Hybrid Coupled Wall (HCW) system, a central RC wall is coupled to two side steel columns with replaceable steel links pinned to the columns. Damaged links are supposed to be replaced after severe ground motions; however, significant residual deformations after strong

earthquakes can challenge the practicality of replacing damaged links.

The implementation of SC coupling beams can be an efficient solution to address the issues related to earthquake-induced residual deformations. Different configurations of SC coupling beams taking advantage of post-tensioned bars/cables have been proposed in literature [9-13]. These configurations are often based on a gap-opening mechanism at beam-to-wall interfaces. The gap is closed after loading due to the restoring force provided by post-tensioned bars/cables. However, beam elongation under large deformations can impair the performance of these SC coupling beams [14].

This paper presents the results of a preliminary numerical study about the seismic performance of an alternative structural system inspired by the coupled system proposed by Zona *et al.* [7] and featuring SC links in the coupling beams. The proposed lateral load-resisting system is referred as Self-Centering Hybrid Coupled Wall (SC-HCW). A friction-damped SC link similar to the one proposed by Huang and Wang [15] is adopted to couple the RC wall to the side steel columns. This link offers the following key

advantages: (i) large and controlled energy dissipation capacity; (ii) self-centering capability; (iii) easy reparability; (iv) eliminates problems related to the coupling beams elongation; (v) facilitates the application of pre-fabricated SC components, which mitigates uncertainties raised by post-tensioning connections on site. An eight-story building is considered for case study purposes and is used to investigate and compare the seismic performance of a SC-HCW and its conventional HCW counterpart. The seismic performance of the SC-HCW is investigated through non-linear static and Incremental Dynamic Analyses (IDAs), and the supremacy of the SC-HCW as an alternative seismic-resisting structural system is highlighted by comparing the results obtained for the SC-HCW and HCW. In addition, fragility curves are developed with respect to Local Engineering Demands (EDPs) for both SC-HCW and HCW to prove the application of the proposed SC links does not aggravate local damages expected for coupled walls.

2 Case study building and HCW/SC-HCW

An eight-story building with the plan view shown in Figure 1(a) was considered as the case study [16]. The permanent (dead) and live gravity loads were assumed equal to 4.5 and 2 kN/m², respectively. The archetype SC-HCW and HCW were designed to form the lateral load-resisting system of the case study building. The elevation view of the HCW/SC-HCW is schematically shown in Figure 1(b).

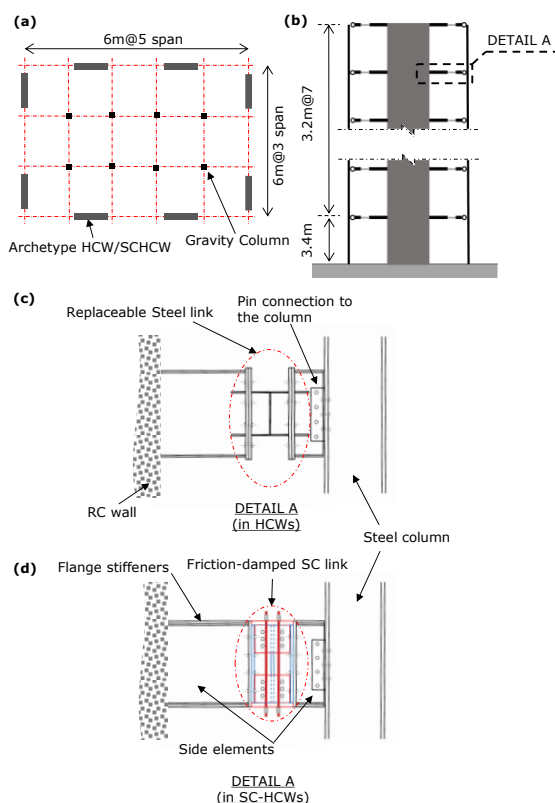


Figure 1 (a) Plan view of the case-study eight-story structure; (b) Elevation view of the HCW/SC-HCW system; (c) Details of coupling beams in the HCW; (d) Details of coupling beams in the SC-HCW

2.1 Design of the HCW and SC-HCW

The design procedure proposed by Zona *et al.* [7] was followed to design both HCW and SC-HCW. Preliminary studies [17] suggested a height-to-width (h/l_w) ratio of 10 for

coupled RC walls. This optimum ratio provides enough flexibility to allow plastic deformations in the steel coupling links, while limiting the excessive lateral deformations. The width of the shear wall, l_w was chosen equal to 3.2 m considering the height of the building in this study. The thickness of the wall was assumed equal to 400 mm. Concrete was considered as class C30 ($f_c' = 30\text{MPa}$), and the reinforcement class was assumed B450C with a yield strength of $f_{yr} = 450\text{MPa}$ in accordance with Eurocode 2 [18]. Reinforcement were detailed to meet the DCM design provisions of Eurocode 8 [19], which resulted in a bending moment capacity of 9500 kNm.

The total overturning moment resisted by the HCW subjected to lateral loading consists of the moment reaction developed at the base of the wall and the coupling action induced by the axial force in the columns. The ratio of the overturning moment resisted by the coupling action to the total overturning moment, *i.e.*, the Coupling Ratio (CR), was chosen equal to 55%, referring to previous studies and values suggested for mid-rise buildings [2]. Setting the CR and having the base moment capacity of the wall, the axial force demand (coupling action) in columns can be evaluated. The links' shear force was then estimated based on the columns' axial force assuming a uniform distribution of shear force among the links along the height of the HCW/SC-HCW.

The coupling beams of the HCW/SC-HCW consist of two side elements and an internal link, as shown in Figure 1(c) and (d). The side elements are designed such that they remain elastic, which allows damage concentration in the links. The links of the HCW are conventional replaceable steel links, and their I-shaped built-up cross-section was designed based on the shear force demand and referring to the requirements suggested by Das *et al.* [8]. These requirements ensure that the link flanges remain elastic while their web yields in shear. Table 1 represents the links' cross-section properties for the HCW.

Table 1 Properties of the built-up links of the HCW

Width [mm]	Depth [mm]	Flange thickness [mm]	Web thickness [mm]	Plastic Shear capacity [kN]	Plastic Bending capacity [kNm]
120	240	20	6.2	225	145

The SC-HCW is equipped with friction-damped self-centering devices similar to the one proposed by Huang and Wang [15] (Figure 1 (d)). In this configuration, vertical post-tensioned (PT) bars provide the restoring force and a friction slip mechanism provides energy dissipation capacity. The SC configuration consists of two T-shaped pieces fixed to the adjacent structural members and two restrainers as indicated in Figure 2. Each restrainer is built up by welding one end of two vertical frictional plates to an horizontal anchorage plate (Figure 2(b)). The top and bottom restrainers are clamped to the T-shaped pieces by four post-tensioning (PT) bars to maintain the integrity of the SC links. Figure 2(a) shows a schematic representation of the SC link configuration, and additional details can be found in Huang and Wang [15]. In order to allow calibration of strength and stiffness of the SC links, the configuration proposed by Huang and Wang was slightly updated in this study by adding disk springs in parallel and series

to the PT bars (Figure 2 (a)). The flag-shaped shear-relative vertical displacement ($V_l - \Delta_l$) behavior of the SC link is schematically represented in Figure 2(d). Under extreme loading, the shear force in the SC links (V_l) can exceed the post-tension in PT bars (F_{PT}) and the frictional resistance between the web of T-shaped pieces and the frictional plates (F_{fr}). Consequently, a gap is opened between the anchorage plates and the T-shaped pieces at opposite corners of the SC links (Figure 2(a)). The shear force at the onset of gap opening is referred as the decompression force ($F_{Dec} = F_{fr} + F_{PT}$). The stiffness of the SC links when the gap is open, K_{eq} , is calculated based on the stiffness of the PT bars and disk springs arranged in parallel and series (Figure 2(a)). Since the elastic stiffness of the PT bars is too high to allow the required gap opens before the PT bars yield, the disk springs are arranged in series to reduce K_{eq} . This also decreases the elastic deformation demand on PT during the gap-opening phase. The SC links were designed to have the same F_{Dec} as the shear force demand estimated earlier for the links of both HCW and SC-HCW. Table 2 presents the SC link properties. It should be noted that the post-activation stiffness of the SC links was chosen deliberately in this study to match the post-yield shear resistance of their counterpart conventional steel links.

Table 2 Properties of the SC links of the SC-HCW

Post-tension force [kN]	F_{fr} [kN]	F_{Dec} [kN]	K_{eq} [kN/mm]
33	70	200	6

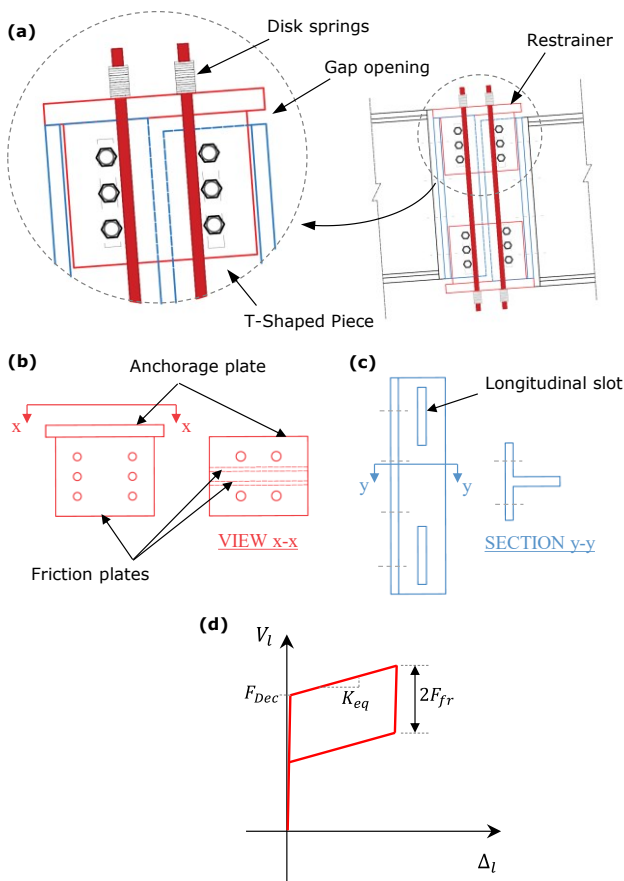


Figure 2 (a) Deformed shape of the SC link; (b) SC link restrainer;

(c) SC link T-shaped piece; (d) Shear force-vertical deformation response of the SC link

3 Finite Element modelling methodology

2D non-linear models of the HCW and SC-HCW were developed in OpenSees [20]. The RC wall was modelled by implementing the Shear-Flexure Interaction Multiple-Vertical-Line-Element-Model (SFI-MVLEM) [21]. This modelling approach is based on a 2D macroscopic fiber-based model formulation and incorporates biaxial constitutive RC panel behaviour. This model accounts for the axial force-shear interaction, which is critical for modelling the RC walls subjected to lateral loading. This modelling approach has been validated for RC walls in coupled systems, and the modelling parameters suggested by Kolozvari *et al.* [22] were implemented in this study. The RC wall was discretized to 19 fibers (panels) across its width to represent the walls' cross-section and the reinforcement arrangement in the boundary and web areas.

'Elastic BeamColumn Elements' in OpenSees were used to model the side elements of the coupling beams as they are designed to remain elastic. In order to account for the elastic shear deformation of the side elements, a zero-length shear spring with a stiffness equal to the shear stiffness of the side elements cross-section is defined at their connection to the wall. The links of the HCW were modeled using 'Two-Nodes Link Elements'. The links' mechanical behavior is determined by the Unidirectional materials assigned to three springs representing the links' degrees of freedom. The axial and flexural springs were assumed elastic, while the shear springs of the Link Elements were modeled as non-linear. The non-linear shear behavior of the links was characterized by Giuffr -Menegotto-Pinto hysteretic model ('Steel 02' material in OpenSees). The modeling parameters were calibrated against the available experimental results [23]. The same modeling approach was implemented for the SC links in SC-HCW. However, the material model assigned to the shear spring of the 'Two-Nodes Link Elements' was replaced with the 'Self-Centering Uniaxial material' in OpenSees to represent the flag-shaped shear-deformation behavior depicted in Figure 2 (d). Detailed finite element models of the intended SC links were generated, and their nonlinear behaviour was simulated under cyclic loading. The modelling parameters used in this study were calibrated against the results of the detailed finite element simulations.

4 Nonlinear dynamic analyses

The seismic performance of the SC-HCW and HCW was investigated by performing nonlinear time-history analyses in OpenSees [24]. Figure 3 shows the roof drift time-histories obtained for both HCW and SC-HCW under the same ground motion record. This record was scaled such that its spectral acceleration at the archetypes' fundamental period matches the Maximum Credible Earthquake (MCE) spectrum developed according to Eurocode 8 [19]. The comparison shows negligible residual drift for the SC-HCW versus the significant residual drift for HCW, highlighting the benefit of the coupled wall configuration proposed in this study.

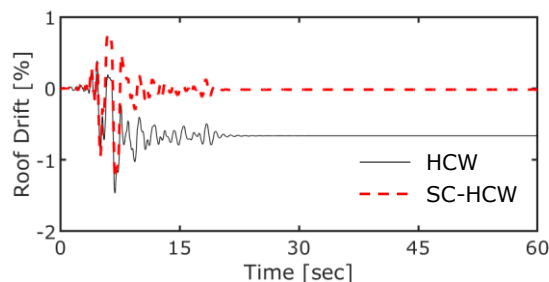


Figure 3 Roof drift time-histories of the SC-HCW and HCW under the same ground motion record

The seismic performance of both structures is also evaluated by IDAs to account for the influence of the record-to-record variability [25]. The 22 pairs of far-field ground motion records suggested by FEMA P695 [26] were used to perform the IDAs. The spectral acceleration at the fundamental period, $Sa(T_1)$, was selected as the Intensity Measure (IM). The fundamental periods of the SC-HCW and HCW were very close, but to allow the comparison of the IDAs results and fragility curves of the two systems the period $T_1=0.9$ sec was selected as the reference fundamental period for the IM definition of both archetypes.

Figure 4 shows the maximum residual interstory drifts for both structures. The medians of the results obtained under 44 ground motion records are represented with solid lines, while the shaded areas represent the variation of the results between 16% and 84% fractiles. Two Damage State (DS) thresholds of the residual interstory drifts suggested by FEMA P-58 [27], $DS1=0.2\%$ and $DS2=0.5\%$, are also superimposed in this figure. DS1 marks the maximum residual interstory drift at which no structural realignment is required for structural stability [27]. While the DS1 limit was not surpassed at MCE intensity level ($IM=1g$) for SC-HCW, more than 16% of ground motions records caused residual interstory drifts larger than DS1 in the HCW. Hence, these results foreground the capability of the friction-based SC link in mitigating the residual deformations, which leads to better reparability and higher seismic-resilience of hybrid coupled walls.

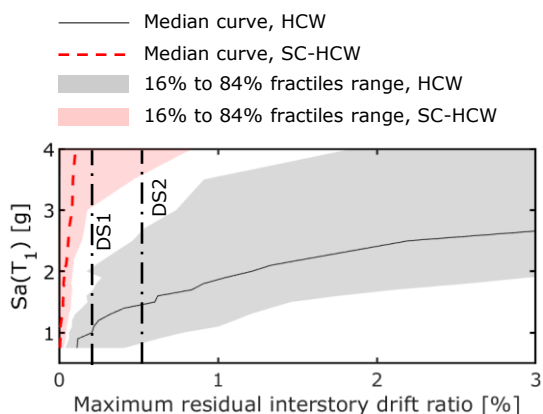


Figure 4 Maximum residual interstory drift ratios

The results of IDAs were also used to develop fragility curves with respect to local Engineering Demand Parameters (EDPs) by fitting a log-normal curve to the fragility data points through least-square minimization. The limit states chosen in this section are directly related to critical component failures, which lead to the system failure in a series arrangement of structural components [28, 29].

The following failure limit states were considered to develop the fragility curves shown in Figure 5:

- Exceedance of links chord rotation limit state ($\theta_{chord,L,ls}$). The capacity limit for this EDP has been set $\theta_{chord,L,ls}$ equal to 0.08 rads, as recommended by Eurocode 8 [19] for short links. Links chord rotation was defined as the ratio of their relative vertical deformation to their width.
- Exceedance of the rebars tensile strain limit state ($\epsilon_{s,ls}^w$) in the RC wall. The capacity limit for this EDP has been set $\epsilon_{s,ls}^w$ equal to 0.05 [30].
- Exceedance of the concrete stress (σ_c) capacity in compression in the RC wall (*i.e.*, concrete crushing). The capacity limit for this EDP has been set equal to the concrete compression strength as defined in the FE model ($\sigma_{c,ls} = f'_c = 33$ MPa for confined concrete in the RC wall boundary regions).

It can be inferred from Figure 5 that the implementation of the SC links did not increase the links chord rotation demand and, consequently the links failure probability.

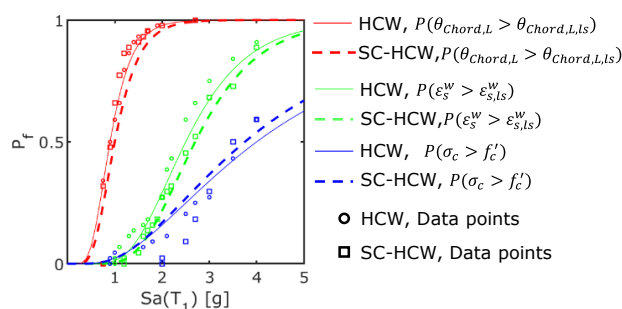


Figure 5 Probability of exceedance of links chord rotation of $\theta_{chord,L,c}$ (red curves); rebars strain of $\epsilon_{s,ls}^w = 0.05$ (green curves); concrete compressive stress of f'_c (blue curves).

The comparison of fragility curves obtained for the SC-HCW and HCW in Figure 5 also confirms that the application of the intended SC links did not affect the probability of exceedance of the two dominant failure modes of RC walls (*i.e.*, reinforcement failure and concrete crushing). Hence, the application of the proposed SC links does not exacerbate earthquake-induced concrete wall damage, while providing SC mechanism and facilitating the repair of hybrid coupled walls after earthquakes.

5 Conclusions

The results of a numerical study about the seismic performance of self-centering hybrid coupled walls (SC-HCWs) were presented in this paper, and the capability of SC-HCWs in eliminating earthquake-induced residual deformations was examined. The supremacy of the performance of an archetype SC-HCW was proved compared with the performance of its conventional hybrid coupled wall (HCW) counterpart. Comparing the results obtained for the intended archetype SC-HCW and HCW highlighted that a significant reduction in residual deformations was achieved by using the self-centering links without exacerbating the damage to the central wall. It is worth-mentioning that the properties of SC links can be calibrated in future studies to even reduce the damage to RC walls and improve the seismic resilience of SC-HCWs. The exceedance of the link chord rotation of the short links rotation

limit (0.08 rads) was the critical failure mode for both archetypes. However, it is worth noting that the configuration of the proposed SC links can allow larger relative vertical deformations or chord rotations. Further experimental studies are required to establish a deformability limit for the proposed SC links. Applying the proposed SC links in structural systems with different configurations and different numbers of stories can also be the subject of future studies.

Acknowledgements

This research was supported by the European Union's Horizon 2020 research and innovation program under grant agreement No. 101027745 (Marie Skłodowska-Curie Research Grant Scheme H2020-MSCA-IF-2020: Self-Centering Earthquake-Resilient Hybrid Steel-Concrete Shear Walls with Rocking Beams - SC-HYBWalls). The Authors also acknowledge the support from the Royal Society - International Exchange programme under the grant agreement IES\R3\213175.

References

- [1] Shahrooz BM;Remmetter ME; Qin F. (1993). Seismic design and performance of composite coupled walls. *Journal of Structural Engineering (United States)*.119(11):3291-309.
- [2] El-Tawil S;Harries KA;Fortney PJ;Shahrooz BM; Kurama Y. (2010). Seismic Design of Hybrid Coupled Wall Systems: State of the Art. *Journal of Structural Engineering*.136(7):755-69.
- [3] Wallace JW;Massone LM;Bonelli P;Dragovich J;Lagos R;Lüders C, et al. (2012). Damage and implications for seismic design of RC structural wall buildings. *Earthquake Spectra*.28(SUPPL.1):S281-S99.
- [4] Kam WY; Pampanin S. (2011). The seismic performance of RC buildings in the 22 February 2011 Christchurch earthquake. *Structural Concrete*.12(4):223-33.
- [5] Wang Y. (2008). Lessons learned from the "5.12" Wenchuan Earthquake: evaluation of earthquake performance objectives and the importance of seismic conceptual design principles. *Earthquake Engineering and Engineering Vibration*.7(3):255-62.
- [6] Westenek B;de la Llera JC;Besa JJ;Jünemann R;Moehle J;Lüders C, et al. (2012). Response of Reinforced Concrete Buildings in Concepción during the Maule Earthquake. *Earthquake Spectra*.28(1_suppl1):257-80.
- [7] Zona A;Degée H;Leoni G; Dall'Asta A. (2016). Ductile design of innovative steel and concrete hybrid coupled walls. *Journal of Constructional Steel Research*.117:204-13.
- [8] Das R;Zona A;Vandoren B; Degée H. (2018). Optimizing the coupling ratio of seismic resistant HCW systems with shear links. *Journal of Constructional Steel Research*.147:393-407.
- [9] Ricles JM;Sause R;Peng SW; Lu LW. (2002). Experimental evaluation of earthquake resistant posttensioned steel connections. *Journal of Structural Engineering*.128(7):850-9.
- [10] Weldon BD; Kurama YC. (2010). Experimental evaluation of posttensioned precast concrete coupling beams. *Journal of Structural Engineering*.136(9):1066-77.
- [11] Zareian MS;Esfahani MR; Hosseini A. (2020). Experimental evaluation of self-centering hybrid coupled wall subassemblies with friction dampers. *Engineering Structures*.214:110644.
- [12] Lettieri A;de la Peña A;Freddi F; Latour M. (2023). Damage-free self-centring links for eccentrically braced frames: development and numerical study. *Journal of Constructional Steel Research*.201:107727.
- [13] Freddi F;Dimopoulos CA; Karavasilis TL. (2020). Experimental Evaluation of a Rocking Damage-Free Steel Column Base with Friction Devices. *Journal of Structural Engineering*.146(10):04020217.
- [14] Deng K;Pan P; Wu S. (2016). Experimental study on a self-centering coupling beam eliminating the beam elongation effect. *The Structural Design of Tall and Special Buildings*.25(6):265-77.
- [15] Huang X; Wang Y. (2021). Development and modelling of new friction damped self-centring link for coupled wall systems. *Engineering Structures*.239:112365.
- [16] Pieroni L;Freddi F; Latour M. (2022). Effective placement of self-centering damage-free connections for seismic-resilient steel moment resisting frames. *Earthquake Engineering & Structural Dynamics*.51(5):1292-316.
- [17] Zona A;Boni P;Degée H;Leoni G;Varelis G;Salvatore W, et al. Innovative hybrid and composite steel-concrete structural solutions for building in seismic area (INNO-HYCO) : final report: Publications Office; 2015.
- [18] 1992-1 E. Eurocode 2: Design of concrete structures. 2004.
- [19] EN1998-1. Eurocode 8: Design of structures for earthquake resistance Brussels2004.
- [20] McKenna F;GL GF;Scott M; Jeremic B. Open System for Earthquake Engineering Simulation (OpenSees). C Berkeley (CA): Pacific Earthquake Engineering Research Center2000.
- [21] Kolozvari K;Orakcal K; Wallace John W. (2015). Modeling of Cyclic Shear-Flexure Interaction in Reinforced Concrete Structural Walls. I: Theory. *Journal of Structural Engineering*.141(5):04014135.
- [22] Kolozvari K;Terzic V;Miller R; Saldana D. (2018). Assessment of dynamic behavior and seismic performance of a high-rise rc coupled wall building. *Engineering Structures*.176:606-20.
- [23] Okazaki T;Arce G;Ryu H-C; Engelhardt Michael D. (2005). Experimental Study of Local Buckling, Overstrength, and Fracture of Links in Eccentrically Braced Frames. *Journal of Structural Engineering*.131(10):1526-35.
- [24] McKenna F;Fenves G;Scott M; Jeremic B. Open System for Earthquake Engineering Simulation (OpenSees). UC Berkeley (CA): Pacific Earthquake Engineering Research Center; 2000.
- [25] Vamvatsikos D; Cornell CA. (2002). Incremental dynamic analysis. *Earthquake Engineering & Structural Dynamics*.31(3):491-514.
- [26] FEMA. Quantification of building seismic performance factors. Washington, DC: FEMA.; 2009.
- [27] Seismic Performance Assessment of Buildings, FEMA P58. Washington, D.C.: Federal Emergency Management Agency; 2018.
- [28] Freddi F;Tubaldi E;Dall'Asta A; Ragni L. Local and Global Response Parameters in Seismic Risk Assessment of RC Frames Retrofitted by BRBs2013.
- [29] Gutiérrez-Urzúa F;Freddi F; Di Sarno L. (2021). Comparative analysis of code-based approaches for seismic assessment of existing steel moment resisting frames. *Journal of Constructional Steel Research*.181:106589.
- [30] Gogus A; Wallace JW. (2015). Seismic Safety Evaluation of Reinforced Concrete Walls through FEMA P695 Methodology. *Journal of Structural Engineering*.141(10):04015002.